Heating-induced conformational change of a novel Î²-(1â3)-D-glucan from Pleurotus geestanus

ARTICLE *in* BIOPOLYMERS · FEBRUARY 2010

Impact Factor: 2.39 · DOI: 10.1002/bip.21303 · Source: PubMed

1 AUTHOR:

Mei Zhang
Case Western Reserve University
39 PUBLICATIONS **1,289** CITATIONS

SEE PROFILE

Heating-Induced Conformational Change of a Novel β-(1→3)-D-Glucan from *Pleurotus geestanus*

Mei Zhang
Department of Chemistry, The Chinese University of Hong Kong, ShaTin, N. T., Hong Kong, People's Republic of China

Received 17 March 2009; revised 9 July 2009; accepted 13 July 2009
Published online 18 September 2009 in Wiley InterScience (www.interscience.wiley.com). DOI 10.1002/bip.21303

ABSTRACT:

Recently, we isolated and purified a neutral polysaccharide (PGN) from edible fungus Pleurotus geestanus. *Its structure was characterized by a range of physical–chemical methods, including high performance anion exchange chromatography, uronic acid, and protein analyses, size exclusion chromatography with ultraviolet, refractive index and light scattering detectors, and nuclear magnetic resonance. Our results revealed that PGN is a novel* β-*(1→3)-D-glucan with glucose attached to every other sugar residues at Position 6 in the backbone. It has a degree of branching of 1/2. Such structure is different from typical* β-*(1→3)-D-glucans* schizophyllan *and* lentinan *in which DB is 1/3 and 2/5, respectively. Rheological study showed a very interesting melting behavior of PGN in water solution: heating PGN in water leads to two transitions, in the range of 8–12.5°C and 25–60°C, respectively. The melting behavior and conformational changes were characterized by rheometry, micro-differential scan calorimetry, atomic force microscopy, static and dynamic light scattering at different temperatures. The first heating-induced transition corresponds to the disintegration of polymer bundles into small helical clusters, resembling the heating-induced dissociation of SPG in water at 7°C; the second one might correspond to the dissociation of helical strands to individual chains. The ability of PGN to undergo a conformation/viscosity transition in water upon heating is very valuable to immobilize cells or enzymes or therapeutic DNA/RNA, which makes PGN a potentially useful biomaterial. © 2009 Wiley Periodicals, Inc. Biopolymers 93: 121–131, 2010.*

Keywords: *polysaccharide; conformation; thermal-sensitive*

This article was originally published online as an accepted preprint. The "Published Online" date corresponds to the preprint version. You can request a copy of the preprint by emailing the Biopolymers editorial office at biopolymers@wiley.com

INTRODUCTION

Poly-branched β-(1→3)-D-glucans as naturally occurring polysaccharides with or without β-(1→6)-D-glucose side chains (6BG3) are integral cell wall constituents in a variety of bacteria, plants, and fungi.[1] *Schizophyllan* (SPG) and *lentinan* (LTN) are this type of glucan with degree of branching (DB) of 1/3[2] and 2/5,[3,4] respectively. This type of polysaccharides has been investigated with great interests because they possess a number of interesting properties. First, 6BG3 stimulate human immune system. Studies show that 6BG3s can activate human macrophages through an interaction with macrophage surface receptor, therefore, they are regarded as immune stimulator and potentiator.[1,5,6] Second, 6BG3s show high viscosity in water with remarkable stability. They are used as a colloidal carrier for trace elements or drugs or industrial viscosity-control agent.[7,8] Third, 6BG3, such as SPG, forms a triple helical structure in water and undergoes a conformational transition upon heating. In 1980s, *Norisuye*

Correspondence to: Mei Zhang; e-mail: rosellezhang@gmail.com
Contract grant sponsor: Hong Kong Special Administration Region (HKSAR) Earmarked Project
Contract grant number: CUHK, GRF404608

clarified that SPG could dissolve in water to form a triple stranded helical structure (t-SPG) at room temperature, but become single-stranded random coil (s-SPG) in dimethylsulfoxide (DMSO).[2,9] The addition of water to the DMSO solution of s-SPG regenerates t-SPG in water via the interstranded hydrophobic interaction and hydrogen bonding.[10] This reversible and highly cooperative transition of SPG has been used to form hybrid complex with nucleic acids and in the formulation of matrices for drug delivery.[11–13]

In searching bioactive polysaccharides from Fungi, we recently isolated and purified a polysaccharide from *Pleurotus geestanus*, labeled as PGN. The structural analysis showed that PGN is a typical 6BG3 polysaccharide with DB of 1/2, different from any other known β-(1→3)-D-glucans including SPG (DB of 1/3) and LTN (DB 2/5). PGN shows some interesting properties. PGN in water shows a gel structure at 4°C, the gel structure is partially dissolved at room temperature, and when the aqueous solution is heated up to 60°C, gel structure is completely dissolved and the solution viscosity remarkably reduced. Such interesting solution property inspired us to investigate PGN, this novel 6BG3, in terms of its structural features, conformations at different temperatures and heating-induced transitions. We believe PGN has great potential to be developed as novel biomaterials as that its thermally sensitive sharp conformation and viscosity changes in water is very valuable to immobilize cell, enzyme, or other therapeutic agents.

EXPERIMENTAL AND PROCEDURES

Preparation of Neutral β-(1→3)-D-Glucan PGN

Edible fungus, *Pleurotus geestanus*, is the source for PGN. The isolation and purification process is briefly described as follows. The fruiting bodies of *Pleurotus geestanus* (Fangshan, Hubei) are immersed in water overnight before they are homogenized. The homogenized fruiting bodies are extracted by hot water for 5 h, centrifuged at 12,000 rpm for 20 min to separate the supernatant and residues. Supernatant is collected, precipitated by 70% ethanol and vacuum dried to obtain the raw polysaccharide. The raw polysaccharide is redissolved in water and fractionated by additional precipitation using ammonium sulfate. The fraction precipitated by 15–20% ammonium sulfate is collected and labeled as PGN for present study.

Monosaccharide Profile

The monosaccharide composition of highly purified PGN after acid hydrolysis was analyzed by high performance anion exchange chromatography (HPAEC) including a Dionex system (Dionex, Sunnyvale, CA) coupled with Carbopac PA1 (4×250 mm^2) and a guard column (3×25 mm^2). The pulsed amerometry with a gold electrode was used for detection. Each solution was clarified by a 0.45-μm filter before its injection into the column. The monosaccharides were separated by the gradient elution from 150 m*M* sodium acetate in 150 m*M* sodium hydroxide (eluent A) to 150 m*M* sodium hydroxide (eluent B). The Dionex AI 450 software was used to control the instrument and collect/analyze data.

Uronic Acid Analysis

The uronic acid content of PGN was determined in dark by a digestion with driselase (Sigma D9515) at 35°C for 48 h. The galactouronic acid and glucouronic acid compositions were analyzed by the HPAEC system. The uronic acids were separated by gradient elution from 500 m*M* sodium acetate in 150 m*M* sodium hydroxide (Eluent A) to 150 m*M* sodium hydroxide (Eluent B).

Protein Analysis

The amount of protein in PGN was determined from its nitrogen content using a NA 2100 protein analyzer (ThermoQuest, CE Instruments). The Eager 200 software was used to control the instrument and collect/analyze the data. The protein content of PGN was further confirmed by a high performance size exclusion chromatography (HPSEC) system with a laser light scattering detector (90°, 633 nm, DAWN DSP-F), ultraviolet (UV) detector (Biosep-SEC-S3000, Phenomenex), as well as an interferometric refractometer (RI, Optilab DSP, Wyatt Technology). The SEC column separates different components according to their molecular size and the scattering intensity of each fraction was measured by LLS detector, leading to its molecular mass. The concentration of each fraction was determined by the RI detector and the protein content the UV detector connected in series.

NMR Spectroscopy

Exchangeable protons were removed by five-time repeated suspending and lyophilizing PGN in D_2O. The spectra were recorded in D_2O using a Bruker Avance 400 spectrometer equipped with a TXI-xyz three-gradient probe and BBO-z gradient probe for the detections of ^1H and ^{13}C, respectively. The one-dimensional (1D)-^1H was measured using the Bruker standard pulse sequence with a frequency of 5000 Hz in 64 K complex data points. The relaxation delay was $5T_1$ to ensure accurate signal integration. Prior to the Fourier transformation, the four-times zero filling and the TRAF function

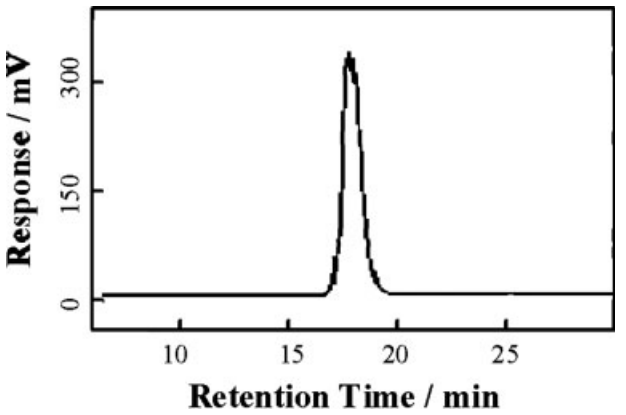

FIGURE 1 Monosaccharide profile of PGN by HPAEC.

were used to reduce the noise. The 1D-^{13}C and 1D-TOCSY spectra was measured using the Bruker standard pulse sequence, respectively, with a frequency of 30,581 and 5000 Hz in 64 K complex data points. For 1D-^{13}C and 1D-TOCSY, the noise was reduced using exponential multiplication. The selective excitation pulse for 1D-TOCSY had a RE-BURP shape. The pulse duration for H-1 at 5.32, 5.28, and 4.98 ppm were set to 40 ms. The two-dimensional (2D)-^{1}H, ^{1}H correlation spectroscopy (COSY) was conducted with 512 increments of 4096 data points with eight scans per t_1 increment using the Bruker standard pulse sequence. The 2D TOCSY was measured with a mixing time for TOCSY spin-lock of 350 ms using the pulse sequence of Griesinger.[14] The 2D-^{1}H, ^{13}C—heteronuclear multiple bond coherence spectroscopy (HMBC) was performed with 256 increments of 2048 data points with 132 scans per t1 increment using the bruker standard pulse sequence.

Temperature Ramp Test

The dynamic moduli as a function of temperature from 4 to 70°C was performed using an ARES rheometer by TA Instruments—Waters LLC (109 Lukens drive, New Castle, DE 19720), equipped with a parallel plate. The maximum strain during oscillation was set to 0.001. The temperature was controlled within 0.1°C by a peltier circulatory system. Evaporation of the sample was prevented by covering the sample with low viscosity silicon oil.

AFM

PGN was dissolved in water by constant stirring at 60°C for 3 h. The PGN solution was kept at 4°C and at room temperature (22°C) overnight, respectively. The 5 μl of PGN solution was pipetted directly onto the newly cleaved mica surface at 4 and 22°C, respectively, then the specimen were dried under these temperatures for 4 h. AFM imaging was performed on a Nanoscope III multimode scanning probe microscope (Digital Instrument) using a piezoelectric scanner. Images were collected using tapping mode AFM. Silicon tips with a spring constant of 42 Nm^{-1} and a resonance frequency of ~320 KHz were used in tapping mode.

Laser Light Scattering

A commercial LLS instrument (ALV 5000) with a vertically polarized 22-mV He-Ne laser head (632.8 nm, Uniphase) was used. The angular range was 6°–155°. The average light scattering intensities of PGN in pure water were determined at the angles of 20°, 30°, 40°, 50°, 60°, 70°, 80°, 90°, 100°, 110°, 120°, 130°, 140°, 150°. The instrument was calibrated with toluene at 25°C as the reference liquid. The specific refractive index increments (dn/dc) was measured using a differential refractometer (BI-DNDC RI Detector, Brookhaven Instruments Corporation, NY) at 632.8 nm for solution at different concentrations in the dilute regime.

RESULTS

Figure 1 shows the monosaccharide composition of PGN by HPAEC, indicating PGN is composed of glucose. The uronic acid analysis (data not shown) showed PGN does not contain uronic acid and is a neutral polysaccharide. No protein was detected in PGN by NA2100 protein analyzer. Figure 2 shows the HPSEC analysis with LLS, RI, and UV detectors. The LLS peak is symmetric and the retention time is consistent with those of RI, indicating the high uniformity of PGN. No elution peak is detected by UV detector, implying that PGN does not contain protein. Table I summarizes the GC-MS results for the analysis of the linkage style of PGN, showing that PGN consists of glucoses connected through (1→3) and (1→6) glycosidic bonds.

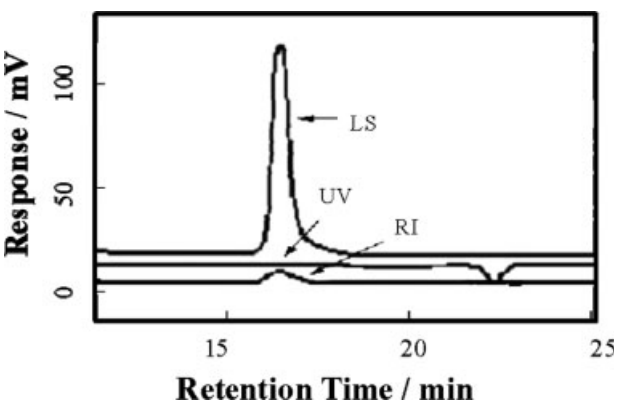

FIGURE 2 The elution profile of PGN by HPSEC couple with LS, RI, and UV detectors.

Table I GC-MS Result of Partially Methylated PGN

Residue	1,5-Di-acetyl-2,3,4,6-tetra-*O*-methyl-hexose	1,3-Di-acetyl-2,4,6-tri-*O*-methyl-hexose	1,3,6-Tri-acetyl-2,4,6-tri-*O*-methyl-hexose
Retention time (min)	25.27	28.36	30.56
Linkage	1→	1→3	1→3,6

Figure 3 shows the ^{1}H NMR spectrum of PGN in D_2O at 60°C. The spectrum contained three signals for anomeric protons at δ 4.95, 5.28, and 5.32, and other sugar protons at δ 3.40–4.24. Figures 4–6 showed the 1D selective TOCSY spectra at three anomeric protons. The 1D selective TOCSY spectra are especially useful for carbohydrate since each sugar ring is discrete spin system separated by oxygen. When an anomeric proton of a sugar ring is selected, the signal is transferred from it to all J-coupled protons in a stepwise process. Figure 7 illustrates the magnetization transfer between protons (Bold) within a sugar spin system. Therefore, Figures 4, 5, and 6 represent spectra of each individual sugar residues in PGN. These three sugar residues were labeled as A, B, and C.

Figure 8 shows the 2D ^{1}H-^{1}H COSY spectrum of PGN in D_2O at 90°C. COSY spectrum correlates protons that are less than three chemical bonds apart because J4 coupling constants are close to zero. For sugar residues A, B, and C, cross peaks between H-1 and H-2, H-2 and H-3, H3 and H4, H4 and H5, H5 and H6a, and H5 and H6b can be observed. The 2D TOCSY experiment (data not shown) correlates all protons of a sugar spin system, in other words, the cross peaks originate from the interaction of all the protons of a sugar residue. A complete series of cross peaks between H-1 and H-2, 3, 4, 5, 6a, and 6b were observed for three sugar residues A, B, and C, respectively. Combining the results of ^{1}H NMR, 1D selective TOCSY, 2D COSY, and 2D TOCSY, the chemical shifts of protons of sugar residues A, B, and C were assigned and summarized in Table II.

Figure 9 shows the 1D ^{13}C NMR spectrum of PGN in D_2O at 90°C. The chemical shifts of carbons are assigned by comparing with ^{13}C NMR spectrum of a well-studied β-(1→3)-D-glucan,[15] revealing that PGN is a typical β-(1→3)-D-glucan. Figure 10 shows the ^{1}H-^{13}C HMBC spectrum of PGN in D_2O at 90°C. The HMBC allows the examination of the linkage style and sequence of sugar residues A, B, and C. In the HMBC spectra, six cross peaks between AC1 and BH3, AC3 and BH1, BC1 and AH3, BC6 and CH1, BC3 and AH1, CC1 and BH6 are assigned to three glycosidic linkages, as indicated by A1→3B, C1→6B, and B1→3A, respectively. Here AC1 represents the Carbon 1 of sugar Residue A, BH3 the Proton 3 of sugar Residue B, etc.

Therefore, our structural analysis indicated that PGN is a typical 6BG3 with DB of 1/2, different from SPG (DB 1/3) and LTN (DB 2/5). Figure 11 illustrates its structure: a β-(1→3)-D-glucan possessing side glucose units on every two sugar residues in the main chain.

This novel PGN shows some interesting thermal sensitive properties. A 0.2% PGN solution in water forms gel at 4°C with good stability; the gel structure is dissolved rapidly and becomes a viscous solution at room temperature; when the solution is heated to 60°C, solution viscosity is largely reduced. Such heating-induced melting of PGN is investigated by rheometry. Figure 12 shows a temperature sweep from 4 to 70°C of 0.2% PGN solution. The temperature dependent storage moduli (G') and loss moduli (G'') have revealed two levels of micro structures, which is different

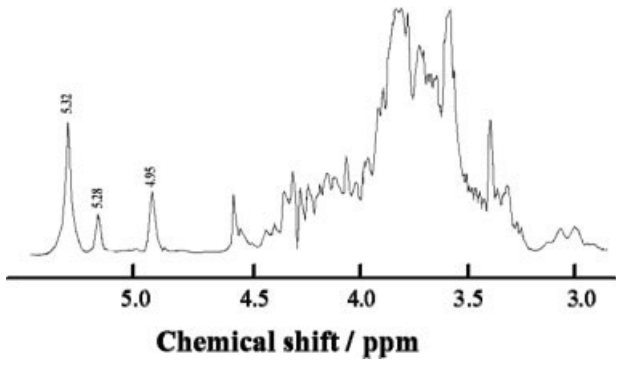

FIGURE 3 The 1D ^{1}H NMR spectrum of PGN in D_2O at 60°C.

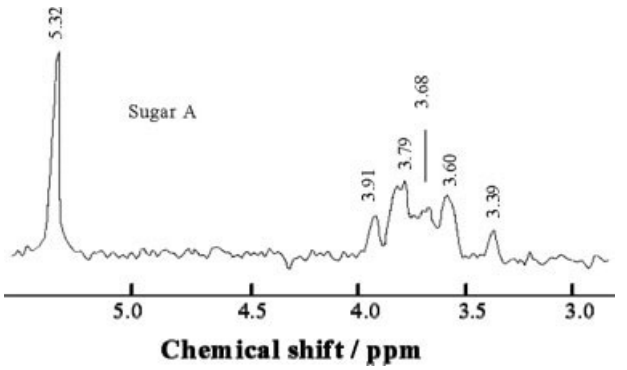

FIGURE 4 The 1D selective TOCSY at 5.32 ppm for sugar A of PGN in D_2O at 60°C.

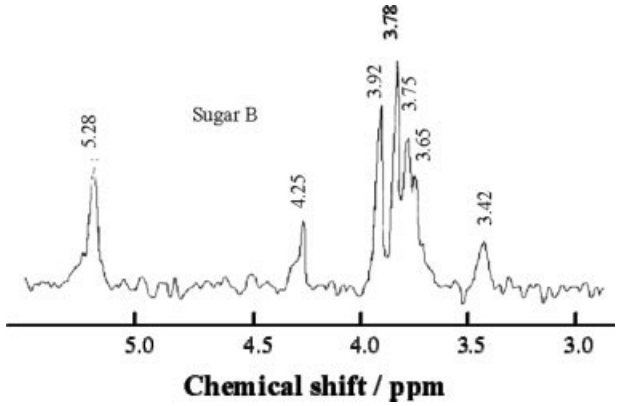

FIGURE 5 The 1D selective TOCSY at 5.28 ppm for sugar B of PGN in D_2O at 60°C.

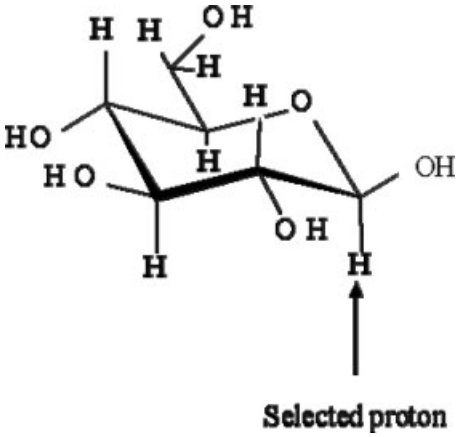

FIGURE 7 Schematic of selective TOCSY of a sugar spin system: the anomeric proton is selected (arrow indicated) and the signal is transferred from selected proton to J-coupled protons (Bold) in a stepwise process.

from other β-(1→3)-D-glucans. The physical gel network starts to melt at 8°C and is gradually weakened in the range of 8–12.5°C. The heating in the range 12.5–25°C has a little effect on the partially melted structure; a further heating to 60°C leads to a disordered state. Such two levels of microstructure and heating-induced transitions were confirmed by an oscillatory frequency sweep at different temperatures, shown in Figure 13. At lower temperatures (4 and 6°C), G′ is independent of the frequency; as the temperature increases in the range 12.5–20°C, G′ slightly increases with the frequency; further increase of the temperature above 40 and 60°C leads to strong frequency dependence of G′, reflecting the relaxation of the components. The cross-over of G′ and G″, as shown in Figure 13 at 60°C, also indicates such relaxation.

The micro-DSC (VP-DSC) was applied to confirm the heating induced transitions in PGN solution in the temperature range from 2 to 130°C. Indeed, Figure 14 shows two enthalpic transitions. The one in the range of 8–12.5°C has an enthalpic change of 8 J g^{-1}; and another in the range of 40–60°C has enthalpic change of 5 J g^{-1}. The micro-DSC trace indicates two-stage transitions from 2 to 130°C.

The microstructures at 4 and 22°C were imaged by AFM. The samples were prepared by depositing and drying their water solution on freshly cleaved mica at 4 and 22°C, respectively. The AFM images were recorded at room temperature. Figures 15a and 15b show the AFM topology graphs of PGN in different scales at 4 and 22°C, respectively, revealing large

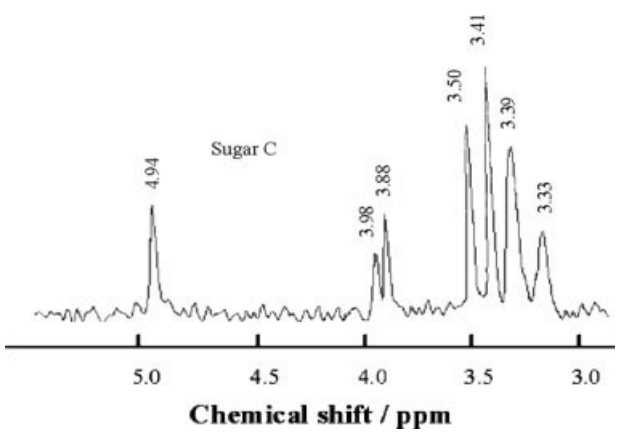

FIGURE 6 The 1D selective TOCSY at 4.95 ppm for sugar C of PGN in D_2O at 60°C.

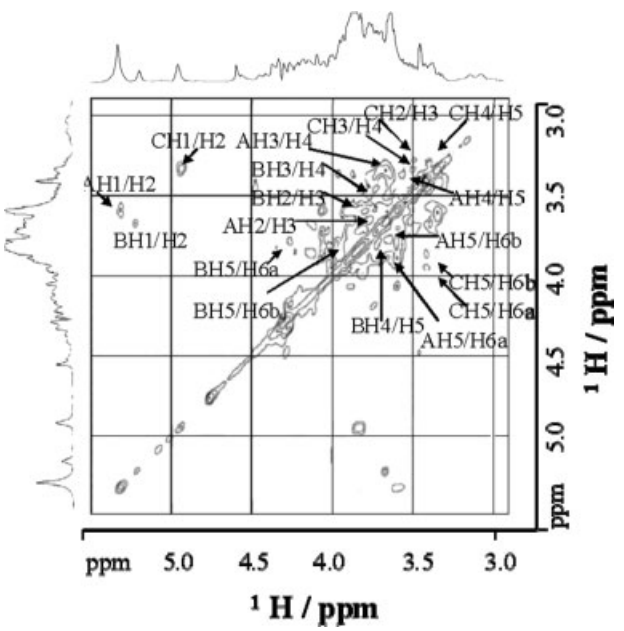

FIGURE 8 The 2D ^1H-^1H COSY spectrum of PGN in D_2O at 90°C. Cross peaks were observed between H-1 and H-2, H-2 and H-3, H-3 and H-4, H-4 and H-5, H5 and H-6a, H-5 and H-6b for three sugar residues A, B, and C.

Table II Chemical Shifts (ppm) of Protons of PGN

	^{1}H/ppm						
Sugar Residue	1	2	3	4	5	6a	6b
A: →3)-β-D-Glcp-(1→	5.32	3.68	3.79	3.39	3.60	3.91	3.82
B: →3,6)-β-D-Glcp-(1→	5.28	3.65	3.78	3.42	3.75	4.25	3.92
C: β-D-Glcp-(1→	4.94	3.39	3.52	3.23	3.41	3.98	3.88

polymer bundles formed at 4°C and much smaller helical structures formed at 22°C. At 22°C, Figure 16 shows the topology graph of PGN at the concentration of 2 mg l^{-1}. Several interesting types of helical structures are observed, including the helical strands formed by more than one PGN chains with approximately equal length (purple circle); the entwined helical strands formed by three or more PGN chains (cyan circle); the cyclic helical strands (red circle). Figure 17 shows the schematic representation on how the helical strands are entangled to form different types of helical structures. Note that the AFM topology images, respectively, at 4 and 22°C, reveal that the microstructure transition in the range 8–12.5°C is related to the disintegration of polymer bundles into small entwined helical strands.

Figure 18 shows the topological graph of PGN at 22°C and the measurement of heights of different areas. The average heights of area (a), (b), and (c) are ∼25, 15, and 5 nm, respectively. The image indicates that more than one PGN chains are twisted into the helical strands. The height of the entwined helical strands (area (a)) is ∼2 times of that of the unentwined helical strand (area (b)), but ∼5 times of that of area (c). This is due to the error of AFM measurements in height.

Further, a sharper AFM tip (radius 5–10 nm) was used to investigate the structural details of PGN helical strand at 22°C. Figure 19 displays a helical structure of PGN, showing the molecular helicity arrays with an inclination angle to the rod axis.

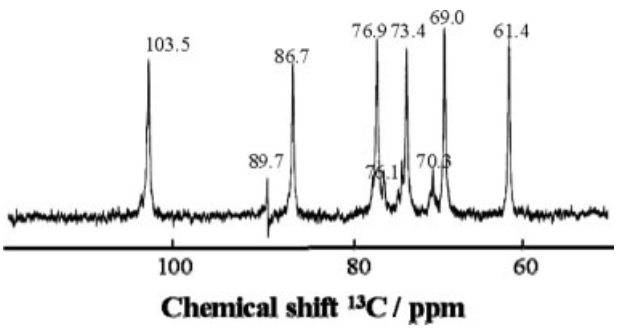

FIGURE 9 The ^{13}C NMR spectrum of PGN in D_2O at 90°C.

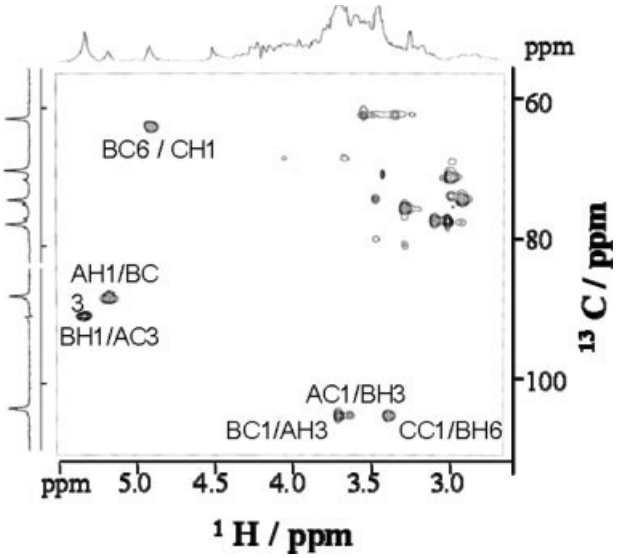

FIGURE 10 The 2D ^{1}H-^{13}C HMBC spectrum of PGN in D_2O at 90°C. Cross peaks were observed between AC1 and BH3, AC3 and BH1, BC1 and AH3, BC3 and CH1, BC3 and AH1, CC1 and BH6. AC1 and BH3, for examples, represent the Carbon 1 of sugar residue A and Proton 3 of sugar residue B.

These images indicate that PGN is a polysaccharide adopts helical strands conformation in solution. However, whether these helical strands are double-helix or triple helix need further investigation such as X-ray diffraction images. AFM was also applied to image PGN structures formed at 60°C. However, AFM images at 60°C are not available because the drying at 60°C on mica substrate was so fast that a significant amount of PGN deposition was lost.

In our investigation, a combination of static and dynamic laser light scattering was used to study the microstructure of PGN at 60°C. Figure 20 shows the scattering vector (q) dependence of $Kc/R(q)$ of a PGN aqueous solution at 60°C,

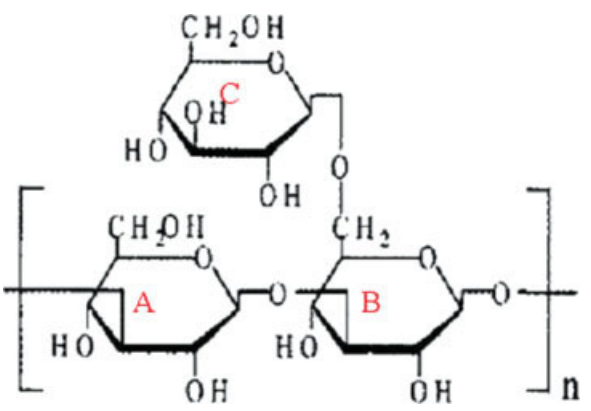

FIGURE 11 The chemical structure of PGN. A, B, and C represent three sugar residues.

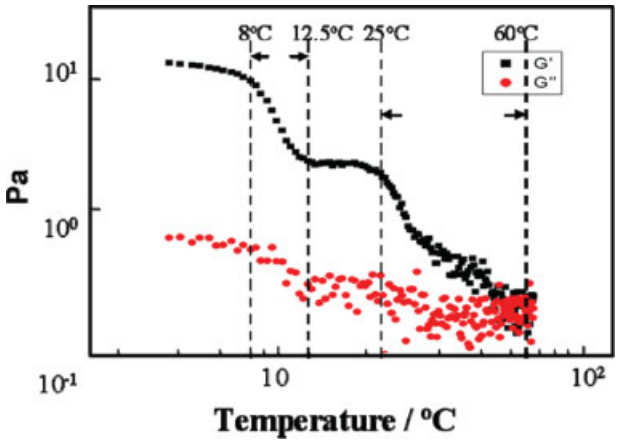

FIGURE 12 Dynamic moduli (G′and G″) as a function of temperature for PGN aqueous solution at 2 mg ml^{-1}. G′, storage modulus; G″, loss modulus; temperature scanning rate 2°C min^{-1}.

where the Rayleigh ratio $R(q)$ is related to the weight-average molar mass (M_w), the z-average mean square root radius of gyration ($\langle R_g \rangle$), and the second viral coefficient (A_2) by:

$$(Kc/R(q))^{1/\alpha} = (1/M_w^{1/\alpha})(1 + (1/3)\alpha \langle R_g^2 \rangle q^2 + (2/\alpha)M_w A_2 c) \quad (1)$$

With $K = (2\pi^2 n^2/N_A \lambda^4)(d_n/d_c)^2$; $q = (4\pi n/\lambda)\sin(\theta/2)$; *and* N_A,λ, n and c being the Avogadro's number, wavelength of the incident laser light in vacuum, the refractive index of solution and solution concentration, respectively. First, we tried the *Zimm* plot, i.e., $\alpha = 1$, but found that $(Kc/R(q))$ vs q^2 was not a straight line even at the low angular range, resulting in unreliable M_w and $\langle R_g \rangle$.[16] Then, the *Berry*[16] plot ($\alpha = 2$) was used so that a linear portion was obtained in the low angular range, shown in Figure 20. The values of M_w and R_g are listed in Table III. The inset of Figure 20 shows the scattering vectors dependence of the average hydrodynamic radius of PGN at 60°C. In dynamic LLS, the Laplase inversion (CONTIN program is used) of a measured time-correlation function can lead to a line width distribution $G(\Gamma)$ that can be further converted to a hydrodynamic radius distribution $f(R_h)$ or an average hydrodynamic radius $\langle R_h \rangle$. Thus obtained R_h is listed in Table III. The $\langle R_g \rangle / \langle R_h \rangle$ is 1.3, implying that PGN has a coiled conformation at 60°C. The transition at 60°C is also indicated by the decrease of the average scattering intensity I(q) and the hydrodynamic radius distribution $f(R_h)$, as shown in Figure 21 and its inset, respectively. The increase of the solution temperature leads to a sharp decrease of I(q) and the shift of $f(R_h)$ to the left, showing an indirect evidence for the heating induced dissociation from helical clusters to coiled chains.

DISCUSSION

The structural analysis by GC, HPLC, uronic acid analysis, HPAEC, and NMR showed that our newly identified PGN is a β-(1→3)-D-glucan with a chemical structure similar to helix-forming polysaccharide SPG, but having a different DB of 1/2. Although a variety of β-glucans differing in primary structures such as DB and degree of polymerization (DP) have been isolated from various fungi sources, this is the first time to obtain and characterize a β-(1→3)-D-glucan with DB of 1/2. It is this different DB that makes PGN showing some interesting heating-induced property that is different from some well studied 6BG3 such as SPG and LTN.

The first transition of PGN in the temperature range of 8–12.5°C is believed to be the disruption of an order

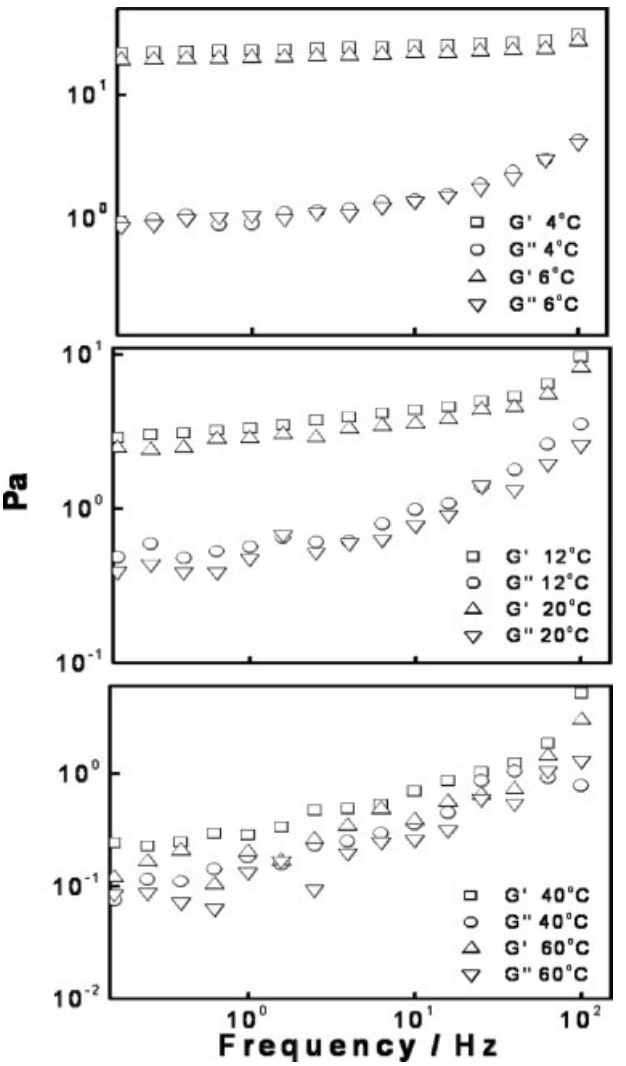

FIGURE 13 Dynamic moduli (G′ and G″) as a function of frequency for PGN aqueous solution at 2 mg ml^{-1} at different temperatures.

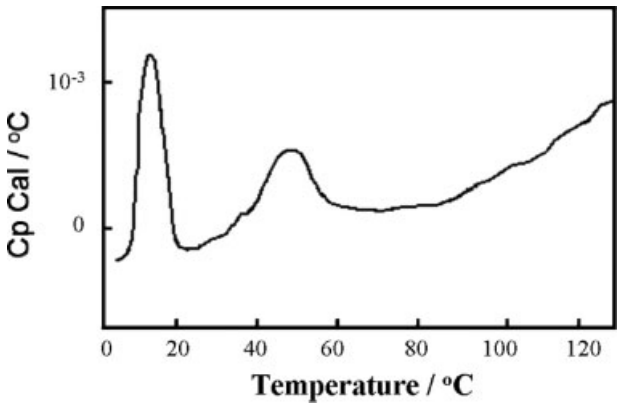

FIGURE 14 The DSC trace for PGN solution at 1 mg ml^{-1} at a scanning rate of 2°C min^{-1}.

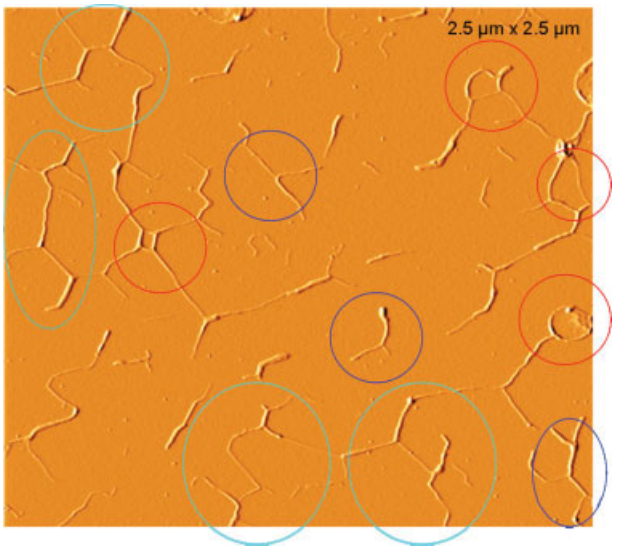

FIGURE 16 The AFM topology graph of PGN at 2 mg l^{-1} at 22°C. Circles of green, blue, cyan, and red represent unimer, helical duplex, duplex cluster, and cyclic helical cluster.

structure organized by side chain residues. As reported, SPG undergoes a state transition around 7°C in water, which is hypothesized by an order-disorder transition in the β-(1→6)-D-glucose lateral residues. These lateral residues, branched from every third glucose unit along each chain, are directed toward the exterior of the SPG helix.[17] Heating from 4 to 7°C leads to a disruption of the ordered organization of lateral residues.[18,19] For our novel PGN, the rheological study and DSC results confirmed a similar transition in the temperature range of 8–12.5°C, which might be caused by the order-to-disorder transition in the lateral residues, i.e., the disruption of the side chain organization. This is well reflected from our AFM images at 4 and 22°C, shown in Figures 15 and 16. At 4°C, the aggregated conformers consist of bundles of polymers, when temperature goes to 22°C, the side chain organization is weakened so that the polymer bundles dissociate into helical strands.

The second transition at ~60°C for PGN, is different from that of ~120°C for SPG. The conformation of PGN at

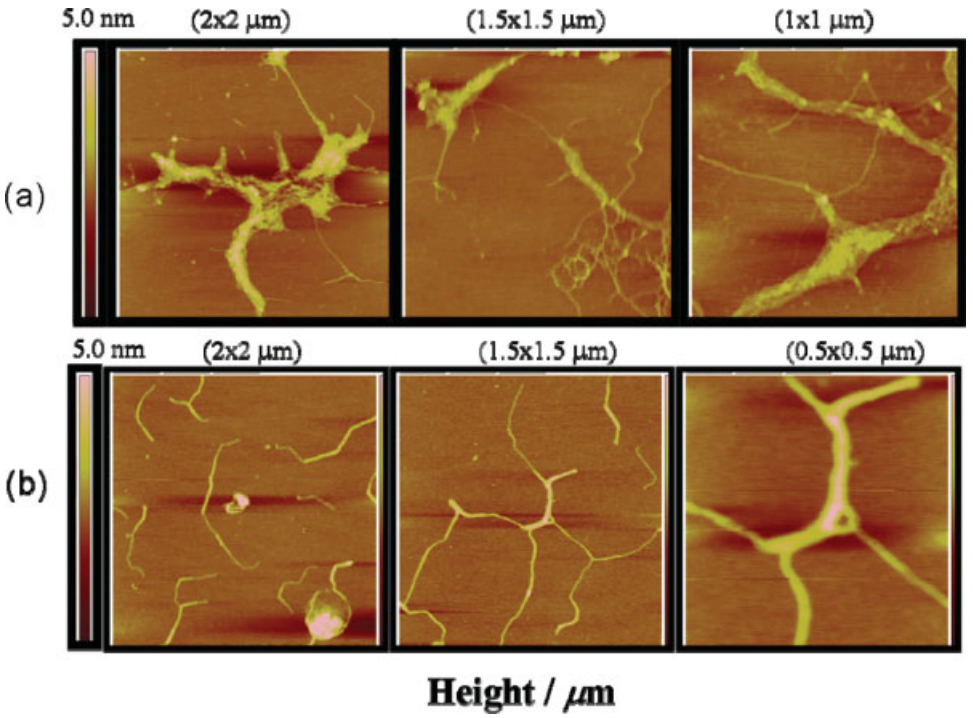

FIGURE 15 The AFM topology graph of PGN at 4 and 22°C.

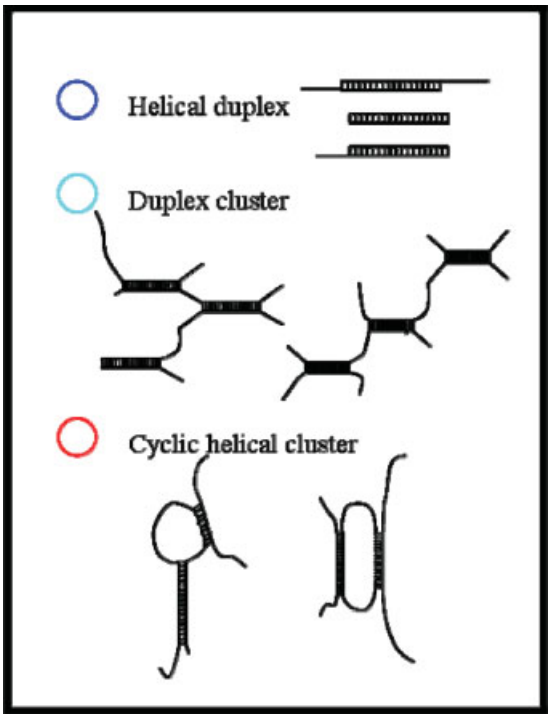

FIGURE 17 Schematic representation of different types of helical structures of PGN.

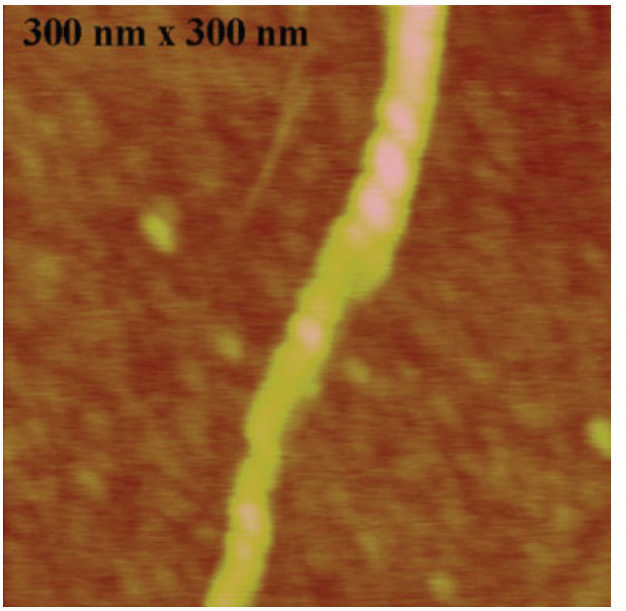

FIGURE 19 An AFM topology graph indicates the helical structure of PGN. Imaged by a shaper tip (tip radius: 5–10 nm) at 22°C.

60°C was failed to be imaged by AFM because the fast vapor evaporation resulted in a significant loss of PGN deposition on mica substrate. Therefore, the transition at 60°C was investigated by laser light scattering because the collapse of the helical strands must be associated with change of scattering light intensity, radius of particle, and the molecular shape. However, the molecular parameters for PGN helical structure at 22°C were not obtained by LLS, due to a relatively broad molecular mass distribution and its structural diversity under this temperature. As shown in Figure 16, the AFM image at 22°C reflects the coexistence of PGN helical strands in different forms. The helical strands entangled helical strands and cyclic helical strands coexist and exhibit different sizes. Besides, the molecular mass distribution of PGN is ∼1.5, indicating that PGN solution contains polymers with a range of sizes. These lead to a broad size distribution of polymer that makes a "messy" contribution to the overall light intensity or dynamic diffusion. In other words, it is not possible to separate either light intensity or dynamic motion of a certain type of particle from the mixture. Therefore, the calculation of molecular parameters of PGN helix at 22°C is not possible. Considering the molecular parameters by LLS at 22°C is not readily available, we investigated the chain conformation of PGN at 60°C and measured light intensity and hydrodynamic radius at both 22 and 60°C to study whether the transition at 60°C corresponds to the change from mixed helical strands to a collapsed state. A largely decreased light intensity and reduced hydrodynamic radius with the increase of temperature indicated a chain collapse from 22 to 60°C. The PGN chain conformation of collapsed state at 60°C was investigated and the molecular parameters were calculated using Berry formulism and shown in Table III. The ratio ($\rho = R_g/R_h = 1.31$) indicates an

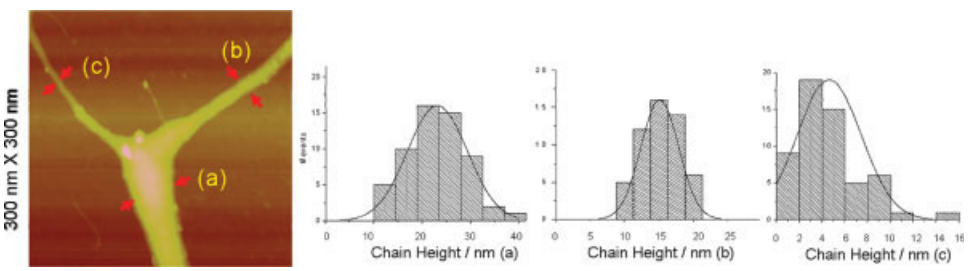

FIGURE 18 The heights measurement of area (a), (b), and (c) of an AFM topology graph at 22°C.

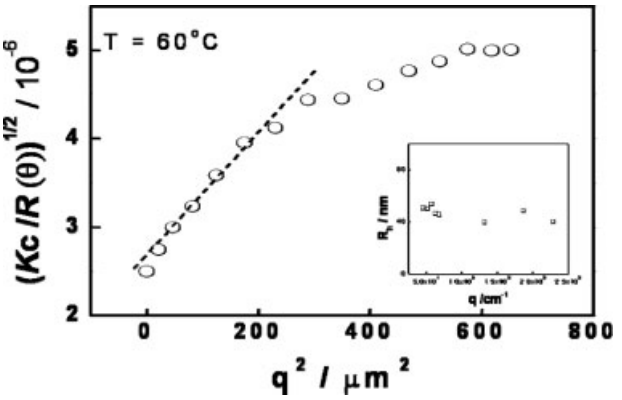

FIGURE 20 The scattering vector (q) dependence of $Kc/R(q)$ of a PGN aqueous solution at 60°C. Inset: The scattering vectors dependence of the average hydrodynamic radius of PGN at 60°C.

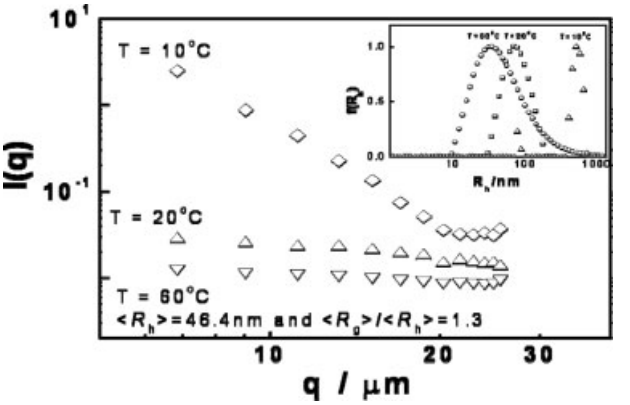

FIGURE 21 The scattering vector (q) dependence of the average scattering intensity I(q). Inset: The R_h distribution of PGN aqueous solution at 10, 20, and 60°C.

expanded coil chain that is much flexible than helical structure, implying that the transition at 60°C might be caused by a collapse from helical structure to coiled chain.

Norisuye and coworkers[18] reported that heating SPG solution at ~120–135°C led to a collapse of triple-stranded helices to single coil. If the transition at 60°C for PGN was caused by helical-to-coil transition, such temperature is much lower than that of SPG. We postulated that the different collapse temperatures of SPG and PGN might be due to the different organization of intermolecular hydrogen bonding network sustained by the secondary hydroxyl groups at Position 2 of glucose units in the main chain. The dependence of melting temperature (T_m) on the number and style of hydrogen bonds is often observed for polynucleotides. For example, more energy is required to disrupt double-stranded DNA with high GC content because GC base pair employs three hydrogen bonds and AT base pair employs two. Our PGN has a different DB (1/2) from SPG (1/3), which might lead to a different organization of inter-stranded hydrogen bonding network and a reduced collapse temperature.

However, further evidences are needed to confirm the PGN helical-to-coil transition at 60°C. Studies of SPG have indicated that the heating-induced disruption of ordered organization of lateral residues is caused by the hydrogen bond association of the side chain glucoses with tightly bound water molecules.[19–23] The strong glucose–water interactions involve hydration layers so that SPG and PGN solutions at 4°C form stable hydrogel structure. Heating their water solution leads to an involvement of fewer tightly bound water molecules and increased rotational freedom of side chain glucose residues. For our PGN solution, there is a possibility that heating to 60°C associates with even fewer or absence of bound water molecules. Although PGN molecular parameters by LLS at 60°C indicate an expanded coiled chain conformation which indicates the transition from helical structure to coils, yet considering PGN is a natural polymer with a relatively broad molecular mass distribution (1.5), we believe the LLS-based analysis needs to be confirmed by some other techniques such as X-ray diffraction. In the present study, we mainly focus on the characterization of this novel polysaccharide PGN and its interesting heating-induced conformational changes.

PGN is a novel β-(1→3)-D-glucan with DB of 1/2 and our preliminary data shows it can specifically bind to immune cells through some surface receptors.[1,2,4,5] Considering the heating-induced property of PGN is very valuable to immobilize cells or enzymes, we believe PGN has great potential to be used as biomaterials for specific delivery of therapeutic DNA/RNA, peptides or drugs to immune cells.

CONCLUSIONS

PGN is a β-(1→6) branched β-(1→3)-D-glucan isolated and purified from fruiting bodies of *Pleurotus geesteranus*. Its M_w and M_w distribution are ~400 K and 1.5, respectively. Different from any known 6BG3 type polysaccharide, PGN has a

Table III The Apparent M_w, Mean Radius of Gyration R_g, Mean Hydrodynamic Radius R_h of PGN Aqueous Solution

Sample	Temperature/°C	Molecular Mass Distribution	M_w (app)	R_g/nm	Mean R_h/nm	$P = R_g/R_h$
PGN	60	1.5	40.1×10^4	62 ± 9.7	46.4 ± 0.7	1.31

degree of branching of 1/2. This different DB leads to some unique solution property of PGN. Heating PGN water solution leads to two transitions, respectively in the range of 8–12.5°C and 40–60°C. The first transition corresponds to the disintegration of polymer bundles to helical strands. Our LLS analysis show the second one might correspond to the dissociation of helical strands to individual PGN chains. Such interesting property makes PGN significant as biomaterial to deliver therapeutic agents because its ability to trigger a sharp transition in conformation and viscosity in aqueous buffer is most valuable to immobilize cells/enzymes/gene drugs.

REFERENCES

1. Vos, A. P.; M'Rabet, L.; Stahl, B.; Boehm, G.; Garssen, J. Crit Rev Immuno 2007, 27, 97–140.
2. Deslanders, Y.; Marchessault, R. H.; Sarko, A. Macromolecules 1980, 13, 1466–1471.
3. Zhang, X.; Zhang, L.; Xu, X. Biopolymers 2004, 75, 187.
4. Xu, X.; Zhang, X.; Zhang, L. Biomacromolecules 2004, 5, 1893–1899.
5. Brown, G. D.; Herre, J. D.; Williams, V.; Willment, J. A.; Marshall, S.; Gordon, S. J Exp Med 2003, 197, 1119–1124.
6. Rogers, N. C.; Slack, E. C.; Edwards, A. D.; Notte, M. A.; Schulz, O.; Schweighoffer, E.; Williams, D. L.; Gordon, S.; Tybulewicz, V. L.; Brown, G. D. Immunity 2005, 22, 507–517.
7. Whistler, R. L.; BeMiller, J. N. Industrial Gums: Polysaccharides and Their Derivatives, 3rd ed.; Academic Press: San Diego, 1995.
8. Fang, C. A.; Takahashi, R.; Nishinari, K. Biomacromolecules 2005, 6, 3202–3208.
9. Sato, T.; Norisuye, T.; Fujita, H. Macromolecules 1983, 16, 185–189.
10. Sakurai, K.; Shinkai, S. J Inclusion Phenomena Macrocyclic Chem 2001, 41, 173–178.
11. Sletmoen, M.; Stokke, B. T. Biopolym 2005, 79, 115–127.
12. Anada, T.; Karinaga, R.; Koumoto, K.; Mizu, M.; Nagasaki, T.; Kato, Y.; Taira, K.; Shinkai, S.; Sakurai, K. J Contr Rel 2005, 108, 529–539.
13. Miyoshi, K.; Uezu, K.; Sakurai, K.; Shinkai, S. Biomacromolecules 2005, 6, 1540–1546.
14. Griesinger, C.; Otting, G.; Wuthrich, K.; Ernst, R. R. J Am Chem Soc 1988, 110, 7870–7872.
15. Tada, R.; Harada, T.; Nagi-Miura, N.; Adachi, Y.; Nakajima, M.; Yadomae, T.; Ohno, N. Carbohydr Res 2007, 342, 2611–2618.
16. Berry, G. C. J Chem Phys 1966, 44, 4550–4556.
17. Takahashi, Y.; Kobatake, T.; Suzuki, H. Rep Prog Pol Phys Jpn 1984, 27, 767–768.
18. Kashiwogi, V.; Norisuye, T.; Fujita, H. Macromolecules 1981, 14, 1220–1225.
19. Itou, T.; Teranoto, A.; Matsuo, T.; Suga, H. Carbohydr Res 1987, 160, 243–257.
20. Hirao, T.; Sato, T.; Teramoto, A.; Matsuo, T.; Suga, H. Biopolym 1990, 29, 1867–1876.
21. Hayashi, Y.; Shinyashiki, N.; Yagihara, S.; Yoshida, K.; Teramoto, A.; Nakamura, N.; Miyazaki, Y.; Sorai, M.; Wang, Q. Biopolym 2002, 63, 21–31.
22. Teramoto, A.; Gu, H.; Miyazaki, Y.; Sorai, M.; Mashimo, S. Biopolym 1995, 36, 803–810.
23. Kony, D. B.; Damm, W.; Stoll, S.; Gunsteren, W.; Hunenberger, P. H. Biophys J 2007, 93, 442–455.

Reviewing Editor: C. Bush